Real-time high-rate co-seismic displacement from ambiguity-fixed precise point positioning: Application to earthquake early warning

Xingxing Li,[1,2] Maorong Ge,[1] Xiaohong Zhang,[2] Yong Zhang,[1,3] Bofeng Guo,[2] Rongjiang Wang,[1] Jürgen Klotz,[1] and Jens Wickert[1]

[1] Nowadays more and more high-rate real-time GPS data become available that provide a great opportunity to contribute to earthquake early warning (EEW) system in terms of capturing regional surface displacements, as an independent information source, useful for promptly estimating the magnitude of large destructive earthquake. In our study, we demonstrate the performance of the real-time ambiguity-fixed precise point positioning (PPP) approach using 5 Hz GPS data collected during El Mayor-Cucapah earthquake (Mw 7.2, 4 April 2010). The PPP-based displacements show to agree with accelerometer-based displacement at centimeter level. The key for successfully obtaining high precision displacements is the efficient ambiguity resolution. PPP with ambiguity fixing can result in correct permanent co-seismic offsets and correct recovery of moment magnitude and fault slip inversion at levels comparable to post-processing.
Citation: Li, X., M. Ge, X. Zhang, Y. Zhang, B. Guo, R. Wang, J. Klotz, and J. Wickert (2013), Real-time high-rate co-seismic displacement from ambiguity-fixed precise point positioning: Application to earthquake early warning, *Geophys. Res. Lett.*, *40*, 295–300, doi:10.1002/grl.50138.

1. Introduction

[2] Earthquake-induced site displacement is key information for locating the epicenter and estimating the magnitude of earthquakes. For earthquake early warning (EEW) systems, the estimation of accurate co-seismic displacements and waveforms is needed in real time. Traditionally, displacements are obtained by double integration of observed accelerometer signals or single integration of velocities observed with broadband seismometers (*Kanamori*, 2007; *Espinosa-Aranda et al.*, 1995; *Allen and Kanamori*, 2003). Compared to seismic instruments that are subject to drifts (accelerometer) or that clip the signal in case of large earthquakes (broadband seismometer), GPS receiver observes displacements directly, making it particularly valuable in case of large earthquakes [*Larson et al.*, 2003; *Blewitt et al.*, 2006].

[3] Mainly two processing strategies are used in real-time or simulated real-time GPS processing: relative baseline/network positioning and precise point positioning (PPP) [*Zumberge et al.*, 1997]. The technique of instantaneous positioning [*Bock et al.*, 2000] is one typical real-time relative positioning method, is integrated into EEW system [*Crowell et al.*, 2009], and is demonstrated by applying the result for centroid moment tensors (CMT) computation [*Melgar et al.*, 2012], finite fault slip inversion [*Crowell et al.*, 2012], and *P* wave detection by combining collocated accelerometer data and the GPS displacements using a Kalman filter [*Bock et al.*, 2011]. The real-time kinematic (RTK) technique is also utilized by *Ohta et al.* [2012] to analyze the displacement of the 2011 Tohoku-Oki earthquake. All of the previously mentioned studies used the relative positioning technique, which is able to guarantee a high accuracy at 1 cm level, but it only provides a relative co-seismic displacement with respect to (at least) one reference station, which might itself be subject to shaking. *Kouba* [2003] demonstrated that PPP using the orbit and clock products of the International Global Navigation Satellite Systems Service (IGS) can be used to detect seismic waves and satisfy the requirement of the GPS seismology. *Wright et al.* [2012] used PPP in real-time mode with broadcast clock and orbital corrections to give station positions every 1 s and then carry out a simple static inversion to determine the portion of the fault that slipped and the earthquake magnitude. The PPP technique can provide "absolute" co-seismic displacements with respect to a global reference frame (defined by the satellite orbits and clocks) with a stand-alone GPS receiver. A PPP processing system uses information from a global reference network, which is applied to the monitoring stations, consequently the derived positions are referred to the global network, which itself is hardly affected by the earthquake displacement. However, it has limited accuracy in real-time applications because of unresolved integer-cycle phase ambiguities [*Li*, 2012].

[4] In recent years, integer ambiguity fixing approach for PPP has been developed to improve its performance [*Ge et al.*, 2008; *Geng et al.*, 2012]. The German Research Center for Geosciences (GFZ), as one of the IGS data analysis centers, is operationally providing GPS orbits and clocks, uncalibrated phase delays (UPDs), and differential code biases (DCBs) for real-time PPP service with ambiguity fixing [*Ge et al.*, 2011; *Li*, 2012]. In this contribution, the ambiguity-fixed PPP method is employed to estimate high-rate co-seismic displacement in real time. Meanwhile, we do not form linear combinations and use only original observables of carrier phases and pseudo-ranges in order to suppress the measurement noise. The slant ionospheric delays are treated as unknown parameters and the temporal

correlation is also considered to strengthen the solution. This original ambiguity-fixed PPP algorithm is described in section 2. The PPP displacement waveforms are analyzed and compared with seismic waveforms in section 3, and the application of PPP waveforms to EEW is described in section 4.

2. GPS Data Processing

[5] From the GPS observational equations (see Supporting Information),[1] one can see that ambiguities cannot be fixed to integers because of the existence of UPDs. The real-valued ambiguities can be expressed by integer numbers and the UPDs at receiver and satellite as

$$B_r^s = N_r^s + b_r - b^s \tag{1}$$

[6] Fortunately, recent studies show that the UPDs can be estimated with high accuracy and reliability from a global reference network and casted for recovering integer ambiguities at the user end [*Ge et al.*, 2008]. Several IGS analysis centers are providing a UPD data product for PPP ambiguity fixing, which can be used for geophysical GPS applications [*Ge et al.*, 2011; *Loyer et al.*, 2012].

[7] Usually an ionosphere-free linear combination of dual-frequency observations is employed in PPP to eliminate the effect of ionospheric delays as a standard technique. In order to suppress the measurement noise, we do not form such linear combination in this contribution [*Schaffrin and Bock*, 1988]. Only original carrier phase and pseudo-range observations at L1 and L2 frequencies are employed and the slant ionospheric delays are estimated as unknown parameters.

[8] At the epoch k, observational equations for all the satellites can be expressed as

$$Y_k = A_k \cdot X_k + \varepsilon_{Y_k}, \varepsilon_Y \sim N(0, \sigma_Y^2) \tag{2}$$

The estimated parameters are

$$X = \left(\Delta r^T \ Z_r \ t_r \ \left(I_{r,1}^s \right)^T \ \left(N_{r,1}^s \right)^T \ \left(N_{r,2}^s \right)^T \right)^T \tag{3}$$

[9] A sequential least square filter is employed to estimate the unknown parameters for real-time processing. P_k denotes the weight matrix at epoch k:

$$\hat{X}_k = P_{\hat{X}_k}^{-1} \cdot \left(A_k^T P_k Y_k + P_{\hat{X}_{k-1}} \hat{X}_{k-1} \right) \tag{4}$$

$$Q_{\hat{X}_k} = P_{\hat{X}_k}^{-1} = \left(A_k^T P_k A_k + P_{\hat{X}_{k-1}} \right)^{-1} \tag{5}$$

[10] The increments of the receiver positions Δr are estimated epoch by epoch without any constraints between epochs for retrieving any rapid motions at the stations. The tropospheric zenith wet delay Z_r is described as a random walk process with noise of about 2–5 mm/$\sqrt{\text{hour}}$. The process noise of receiver clock t_r is set to white noise. The carrier-phase ambiguities $N_{r,j}^s$ are assumed to be constant over time. The L1 and L2 ambiguities are fixed simultaneously using the LAMBDA method by *Teunissen* [1995]. The line-of-sight ionospheric delays $I_{r,1}^s$ are taken as estimated parameters for each satellite and at each epoch. A temporal constraint is introduced to strengthen the solution:

$$I_{r,t}^s - I_{r,t-1}^s = w_t, w_t \sim N(0, \sigma_{wt}^2) \tag{6}$$

[11] Here w_t is the ionospheric change from the previous to the current epoch. σ_{wt}^2 is the variance of w_t (generally a few millimeters for the 5 Hz data sampling) and an elevation-dependent weighting strategy is applied.

3. PPP Displacements

[12] The 2010 *Mw* 7.2 El Mayor-Cucapah earthquake (4 April 2010, 22:40:42 UTC) in northern Baja California provides us with a real event to evaluate the performance of real-time PPP-derived co-seismic displacements. We process 1 Hz data of about 80~90 real-time IGS stations using the EPOS-RT software of GFZ in simulated real-time mode (in a strictly forward direction) for providing GPS orbits and clocks (about 0.1 ns accuracy), UPDs, and DCBs at 5 Hz sampling rate. Based on these real-time corrections, we replay 5 Hz GPS data collected by 30 stations of the California Real Time Network (CRTN). Displacement waveforms are computed on a
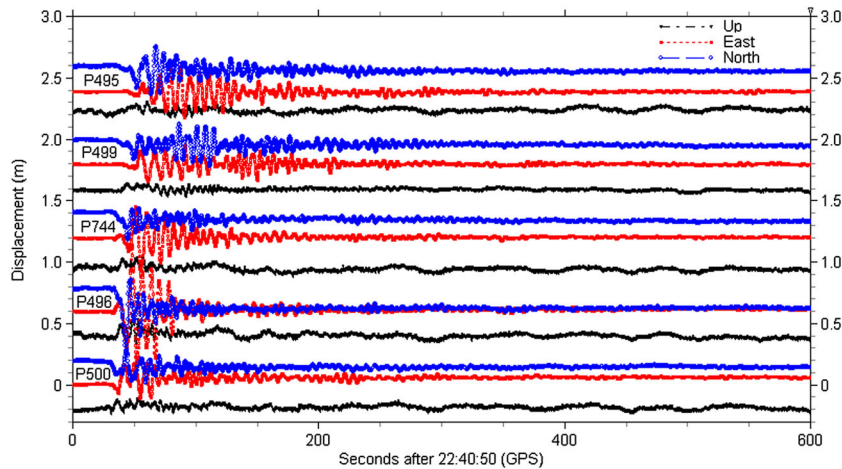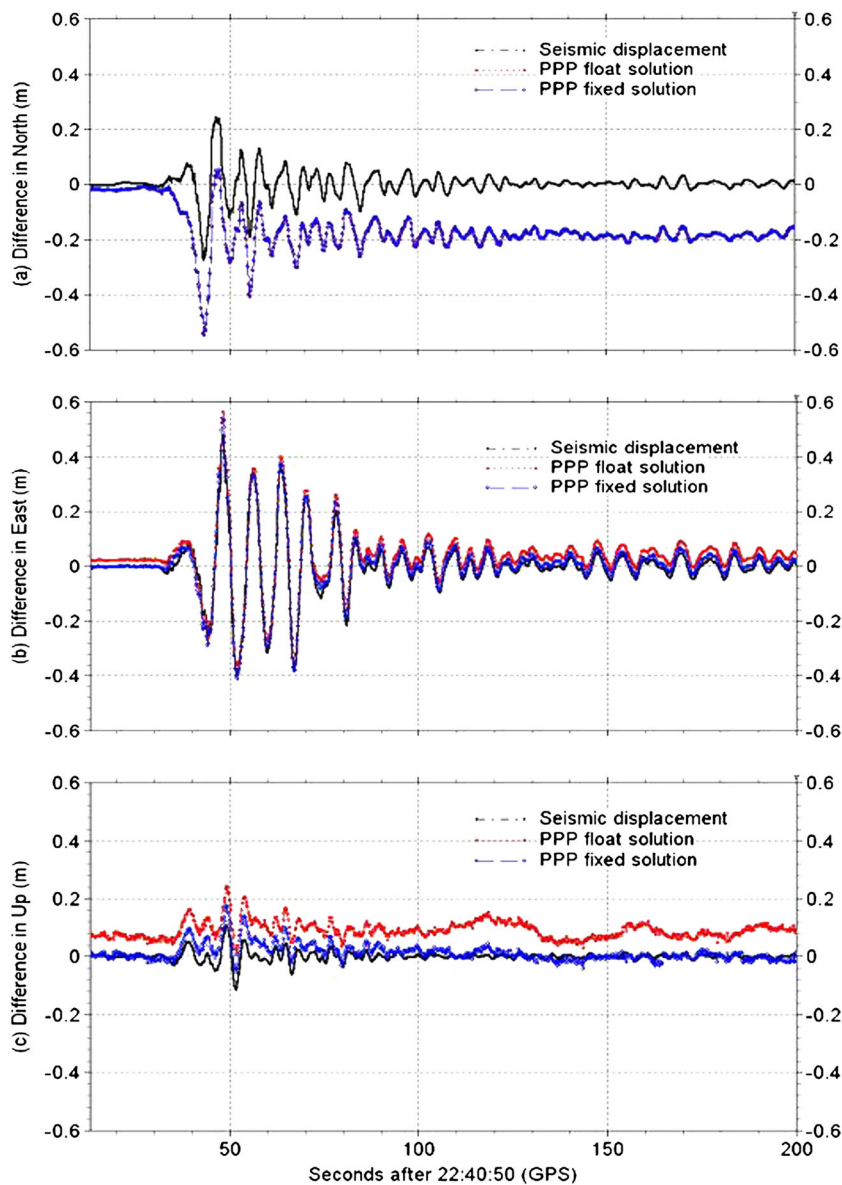

Figure 1. PPP displacement waveforms at GPS stations of P495, P499, P744, P496, and P500 during the El Mayor-Cucapah earthquake on 4 April 2010. The north, east, and up components are respectively shown by blue curve, red rectangle, and black triangle.

station-by-station basis using the proposed original ambiguity-fixed PPP algorithm in section 2, in a simulated real-time mode (in a strictly forward direction). The displacement results of five stations are shown as examples in Figure 1.

[13] Some of the GPS stations are co-located with seismic stations from the Southern California Seismic Network (SCSN) operated by the USGS (U.S. Geological Survey) and Caltech. Velocity and displacement waveforms can be obtained from accelerometer data through single and double integrations, respectively. PPP displacements are compared with those from the accelerometers at these co-located stations. The GPS station P496, which is located ~60 km from the earthquake's epicenter, is co-located with the SCSN seismic station 5058 (about 140 m distance). Comparisons of the seismic and PPP displacement waveforms for these stations are shown in Figure 2.

[14] In Figure 2a, the north component shows a high degree of resemblance, with aligned phase and very similar amplitudes of the dynamic component. The difference is that a permanent co-seismic offset in the north component of 0.2 m in the PPP waveforms is clearly visible. Tilt and rotation of the seismic instrument result in distortions and baseline offsets, thus permanent co-seismic offsets are lost in the seismic waveforms. Figure 2b displays an excellent agreement of seismic and PPP displacements in the east component within few centimeters. The vertical is, as expected, the noisiest component, due to the satellite constellation configuration and the high correlation between zenith tropospheric delay and the height component. PPP float solution is also shown in the same figure and the comparisons indicate that integer ambiguity fixing can improve the accuracy of real-time PPP displacements significantly
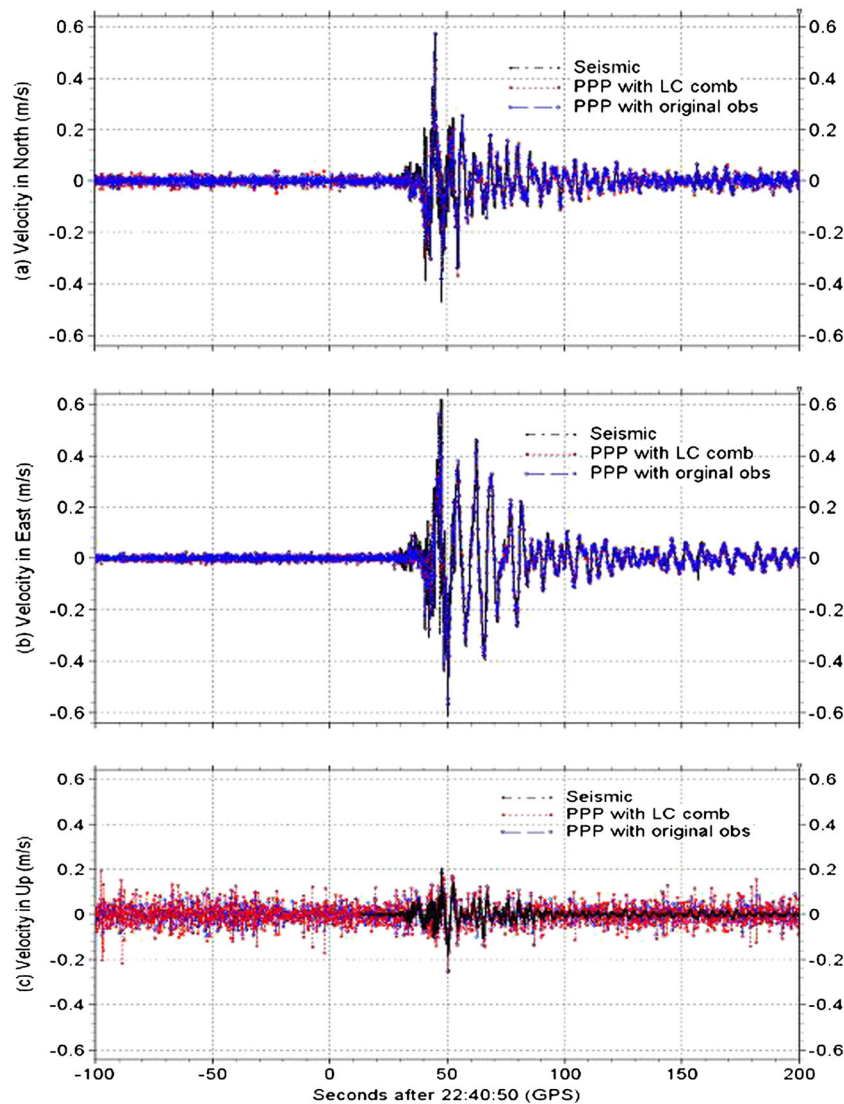

Figure 2. Comparisons of the seismic and PPP displacement waveforms on the co-located 5058 (seismic) and P496 (GPS) stations during the El Mayor-Cucapah earthquake on 4 April 2010 with the (a) north, (b) east, and (c) up components. The real-time ambiguity-fixed PPP waveform estimated from GPS observations is shown by the blue curve. The seismic displacement waveform integrated (twice) from accelerometers is drawn by the black triangle. The traditional PPP float solution is also shown for comparisons with the red rectangle.

especially in the east component. We calculated the root mean square (RMS) values of 2 h (before the earthquake event) position series of the 30 GPS stations. The accuracy $(1 - \text{sigma})$ of the PPP float solution is found to be 2.2, 4.1, and 7.6 cm, respectively, in north, east, and up direction. PPP ambiguity fixing can improve the accuracy to 1.8 cm, 1.9 cm, and 3.9 cm in the corresponding directions.

[15] The velocity series of five stations are shown in Figure S1 of the Supporting Information. These series, derived from PPP are compared with those integrated from a nearby accelerometer, and the results for 5058/P496 are exemplarily shown in Figure 3. The velocity series derived from original PPP fixed solution are shown by the blue curve, while the corresponding results integrated from accelerometers are shown by the black triangle. A statistical analysis indicates that their difference $(1 - \text{sigma})$ is 2.1, 2.0, and 3.1 cm/s in north, east, and height component,

respectively. From Figures 3a and 3b, the velocity series in the horizontal component show a high degree of consistency with the corresponding seismic results. Figure 3c indicates that the vertical component is relatively noisy. The velocity series, derived from ionosphere-free PPP fixed solution are also plotted with red rectangles. It is visible that the use of original carrier phases and pseudo-ranges can suppress the noise and improve the PPP precision. The statistical difference between the ionosphere-free PPP and seismic results is 2.5, 2.3, and 4.0 cm/s, respectively, in north, east and up direction. We also calculated the RMS values of 2 h (before the earthquake event) velocity series for the 30 GPS stations. The corresponding accuracy $(1 - \text{sigma})$ of these series derived from ionosphere-free PPP fixed solution are found to be 1.6, 0.9, and 4.6 cm/s, respectively, in the north, east, and up direction. The proposed method of using original observables for PPP ambiguity fixing can suppress the noise and improve

Figure 3. Comparisons of the velocity series from PPP and accelerometer on the co-located 5058 (seismic) and P496 (GPS) stations during the El Mayor-Cucapah earthquake on 4 April 2010 with the (a) north, (b) east, and (c) up components. The blue curve shows the velocity series derived from the PPP fixed solution where original observations are employed. The black triangle shows the corresponding results integrated from accelerometers. The velocity series derived from the traditional PPP fixed solution where ionosphere-free combinations are employed are also shown for comparisons with the red rectangle.

the accuracy to 1.2, 0.7, and 4.0 cm/s in the corresponding directions.

4. Application to Earthquake Early Warning

[16] We demonstrated here the performance of earthquake early warning using the real-time ambiguity-fixed PPP approach. The important information, provided by the PPP position series is the permanent displacement. We use the real-time algorithm proposed by *Allen and Ziv* [2011] to remove dynamic oscillations and extract these displacements. The horizontal components of the results (about 1 min after *S* wave arrival) are shown in Figures S2 and S3.

[17] We derived three fault slip distributions from the co-seismic displacements calculated from the real-time PPP float solution, real-time PPP fixed solution, and the post-processed daily solution, respectively. For this purpose, we used the code written by one of the co-authors (R. Wang) based on the constrained least-squares method [*Wang et al.*, 2011; *Xu et al.*, 2010]. The fault geometric parameters (strike 313°/dip 88°) are adopted from the global centroid moment tensor (CMT) solution of the earthquake. The rake

angle (slip direction relative to the strike) is allowed to vary ±20° around the CMT solution of 186°. The fault size is 130 km along the strike and 20 km along the dip, which is then divided into $26 \times 4 = 104$ sub-faults. To avoid unreasonable slip patterns, the smoothing constraint is imposed [*Harris and Segall*, 1987]. The inversion results are shown in Figure 4. The three inversions result in scalar seismic moments of 5.35×10^{19} N m, 7.56×10^{19} N m, and 7.58×10^{19} N m, equivalent to moment magnitudes of *Mw* 7.09, *Mw* 7.19, and *Mw* 7.19, respectively. The PPP float solution leads to an underestimation of about 30% of the scalar seismic moment, and PPP fixed solution significantly improves it. Integer ambiguity resolution brings the PPP moment magnitude into agreement with the post-processed value. We conclude that integer ambiguity fixing in PPP is beneficial for fault slip inversion and the moment magnitude estimation in EEW system.

[18] The moment magnitude of the earthquake we estimated in this study is similar to that determined by *Crowell et al.* [2012], and significantly larger than *Mw* 6.8–7.0 obtained by *Allen and Ziv* [2011]. Also our slip pattern is consistent with that obtained by *Crowell et al.* [2012], both
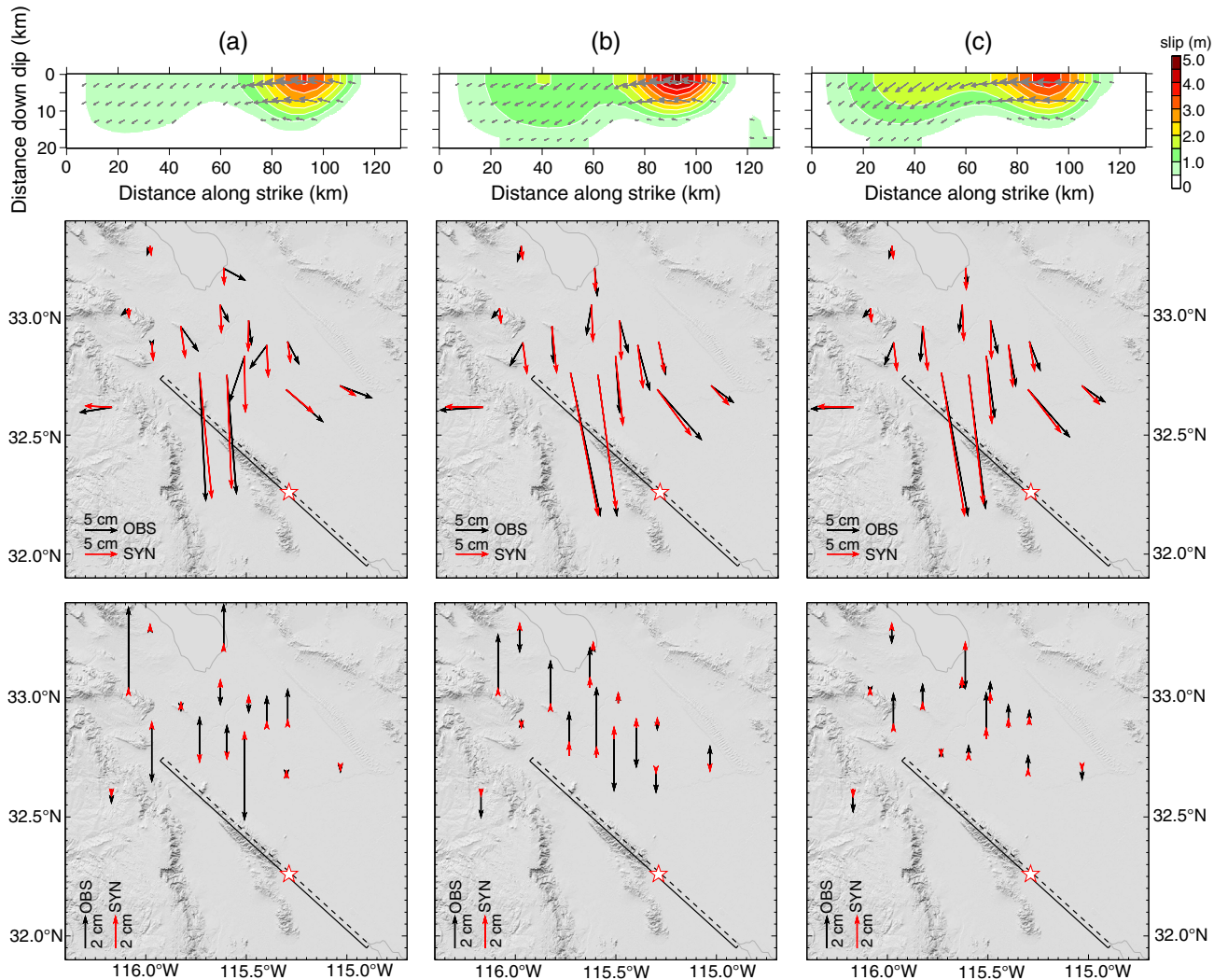
Figure 4. Fault slip inversion with (a) permanent displacements obtained from real-time PPP float solution, (b) real-time PPP fixed solution, and (c) post-processed daily solution. From top to bottom rows are the inverted fault slip distributions, the comparisons of observed and synthetic displacements on horizontal components, and on vertical components, respectively.

showing that the fault slip distributes mainly in shallow depth (0–15 km). However, our peak slip is about 4.0 m that is two times larger than that estimated by *Crowell et al.* [2012]. It is known that the peak slip value depends strongly upon the smoothing constraint used in the inversion. Actually, the slip distribution given by *Crowell et al.* [2012] appears smoother than ours.

5. Conclusions

[19] The PPP technique can provide "absolute" co-seismic displacements with respect to a global reference frame with a stand-alone GPS receiver. In this paper, we present an approach of using real-time ambiguity-fixed PPP for earthquake early warning. The 2010 *Mw* 7.2 El Mayor-Cucapah earthquake was used to evaluate our approach for possible use in EEW.

[20] Comparisons of the displacements, estimated from PPP and accelerometers, displayed a high agreement within few centimeters. Integer ambiguity fixing can improve the accuracy of real-time PPP displacements significantly, especially in the east component. The use of original carrier phases and pseudo-ranges can also suppress the noise and improve the precision of real-time PPP. The results of the fault slip inversions indicate that the real-time ambiguity-fixed PPP can improve fault slip inversion and the moment magnitude estimation and become complementary to existing seismic EEW methodologies.

References

Allen, R., and H. Kanamori (2003), The potential for earthquake early warning in Southern California, *Science*, *300*, 786–789.
Allen, R., and A. Ziv (2011), Application of real-time GPS to earthquake early warning, *Geophys. Res. Lett.*, *38*(16), L16, 310.
Blewitt, G., C. Kreemer, W. C. Hammond, and H. P. Plag (2006), Rapid determination of earthquake magnitude using GPS for tsunami warning systems, *Geophys. Res. Lett.*, *33*, L11309, doi:10.1029/2006GL026145.
Bock, Y., R. Nikolaidis, P. J. de Jonge, and M. Bevis (2000), Instantaneous geodetic positioning at medium distances with the global positioning system, *J. Geophys. Res.*, *105*, 28,233–28,253.
Bock, Y., D. Melgar, and B. W. Crowell (2011), Real-time strong-motion broadband displacements from collocated GPS and accelerometers, *Bull. Seismol. Soc. Am.*, *101*(5), doi:10.1785/0120110007.
Crowell, B., Y. Bock, and M. Squibb (2009), Demonstration of earthquake early warning using total displacement waveforms from real time GPS networks, *Seismol. Res. Lett.*, *80*, 772–782, doi 10.1785/gssrl.80.5.772.
Crowell, B. W., Y. Bock, and D. Melgar (2012), Real-time inversion of GPS data for finite fault modeling and rapid hazard assessment, *Geophys. Res. Lett.*, *39*, L09305, doi:10.1029/2012GL051318.

Espinosa-Aranda, J., A. Jimenez, G. Ibarrola, F. Alcantar, A. Aguilar, M. Inostroza, and S. Maldonado (1995), Mexico City seismic alert system, *Seismol. Res. Lett.*, *66* (6), 42–53.
Ge, M., G. Gendt, M. Rothacher, C. Shi, and J. Liu (2008), Resolution of GPS carrier-phase ambiguities in precise point positioning (PPP) with daily observations, *J. Geodesy*, *82*(7), 389–399, doi:10.1007/s00190-007-0187-4.
Ge, M., J. Dousa, X. Li, M. Ramatschi, and J. Wickert (2011), A novel real-time precise positioning service system: Global precise point positioning with regional augmentation, in: Proceedings of the 3rd Int. Colloquium-Galileo Science, 31 August to 2 September 2011, Copenhagen, Denmark, 2011.
Geng, J., C. Shi, M. Ge, A. H. Dodson, Y. Lou, Q. Zhao, and J. Liu (2012), Improving the estimation of fractional-cycle biases for ambiguity resolution in precise point positioning, *J. Geodesy*, *86*, 579–589, doi:10.1007/s00190-011-0537-0.
Harris, R., and P. Segall (1987), Detection of a locked zone at depth on the Parkfield, California segment of the San Andreas fault, *J. Geophys. Res.*, *92*, 7945–7962.
Kanamori, H. (2007), Real-time earthquake damage mitigation measures. In: *Earthquake Early Warning Systems*, Eds. P. Gasparini, G. Manfredi, and J. Zschau, 1–8. Berlin and Heidelberg: Springer (ISBN-13 978-3-540-72240-3).
Kouba, J. (2003), Measuring seismic waves induced by large earthquakes with GPS, *Stud. Geophys. Geod.*, *47*, 741755.
Larson, K., P. Bodin, and J. Gomberg (2003), Using 1-Hz GPS data to measure deformations caused by the Denali fault earthquake, *Science*, *300*, 1,421–1,424.
Li, X. (2012), Improving real-time PPP ambiguity resolution with ionospheric characteristic consideration. Proc. of ION GNSS-12, Institute of Navigation, Nashville, Tennessee, September,17-21.
Loyer, S., F. Perosanz, F. Mercier, H. Capdevilleet, and J. Marty (2012), Zero-difference GPS ambiguity resolution at CNES-CLS IGS Analysis Center, *J. Geodysey*, *2012*, doi: 10.1007/s00190-012-0559-2.
Melgar, D., Y. Bock, and B. W. Crowell (2012), Real-time centroid moment tensor determination for large earthquakes from local and regional displacement records, *Geophys. J. Int.*, *188*, 703–718, doi: 10.1111/j.1365-246X.2011.05297.x.
Ohta, Y., T. Kobayashi, H. Tsushima, S. Miura, R. Hino, T. Takasu, H. Fujimoto, T. Iinuma, K. Tachibana, and T. Demachi (2012), Quasi real-time fault model estimation for near-field tsunami forecasting based on RTK-GPS analysis: Application to the 2011 Tohoku-Oki earthquake (Mw 9.0), *J. Geophys. Res.*, *117*(B2), B02,311.
Schaffrin, B., and Y. Bock (1988), A unified scheme for processing GPS dual-band phase observations, *Bull. Geod.*, *62* pp. 142–160.
Teunissen, P. J. G. (1995), The least squares ambiguity decorrelation adjustment: A method for fast GPS integer estimation, *J. Geodysey*, *70*, 65–82, 1995.
Wang, R., B. Schurr, C. Milkereit, Zh. Shao, and M. Jin (2011), An improved automatic scheme for empirical baseline correction of digital strong-motion records, *Bull. Seismol. Soc. Am.*, *101*(5), 2029–2044, doi: 10.1785/0120110039.
Wright, T. J., N. Houlié, M. Hildyard, and T. Iwabuchi (2012), Real-time, reliable magnitudes for large earthquakes from 1 Hz GPS precise point positioning: The 2011 Tohoku-Oki (Japan) earthquake, *Geophys. Res. Lett.*, *39*, L12302, doi:10.1029/2012GL051894.
Xu, C., Y. Liu, Y. Wen, and R. Wang (2010), Coseismic slip distribution of the 2008 Mw 7.9 Wenchuan earthquake from joint inversion of GPS and InSAR data, *Bull. Seismol. Soc. Am.*, *100*(5B), 2736–2749, doi: 10.1785/0120090253.
Zumberge, J. F., M. B. Heflin, D. C. Jefferson, M. M. Watkins, and F. H. Webb (1997), Precise point positioning for the efficient and robust analysis of GPS data from large networks, *J. Geophys. Res.*, *102*(B3), 5005–5017, doi:10.1029/96JB03860.